

Supporting Information

Coligand effects on the architectures and magnetic properties of octahedral cobalt(II) complexes with easy-axis magnetic anisotropy

Yuewei Wu,^{a#} Jing Xi,^{a#} Jinhui Yang,^a Weiming Song,^a Shuchang Luo,^{*b} Zheng Wang^a and Xiangyu Liu^{*a c}

^a State Key Laboratory of High-efficiency Utilization of Coal and Green Chemical Engineering, National Demonstration Center for Experimental Chemistry Education, College of Chemistry and Chemical Engineering, Ningxia University, Yinchuan 750021, China

^b School of Chemical Engineering, Guizhou University of Engineering Science, Bijie, 551700, China

^c State Key Laboratory of Coordination Chemistry, Nanjing University, Nanjing, 210023, China.

These authors contributed equally to this work.

***Corresponding author**

Dr. Xiangyu Liu

E-mail: xiangyuliu432@126.com

***Corresponding author**

Dr. Shuchang Luo

E-mail: luosc@gues.edu.cn

Table of contents

Table S1 Selected crystallographic data for complexes **1** and **2**.

Table S2 Selected Bond Lengths (\AA) and Bond Angles ($^\circ$) for **1**.

Table S3 Selected Bond Lengths (\AA) and Bond Angles ($^\circ$) for **2**.

Table S4 Co(II) ion geometry analysis of **1** and **2** by SHAPE 2.1 software.

Table S5 Relaxation fitting parameters from least-squares fitting of $\chi(f)$ data under 2000 Oe dc field of **2**.

Table S6 ORCA/CASSCF computed Individual contributions to *D*-tensor for complex **1**.

Table S7 Energy levels (cm^{-1}) of ligand field multiplets in zero field derived from ORCA/CASSCF computed for complex **1**.

Table S8 ORCA/CASSCF computed Individual contributions to *D*-tensor for complex **2**.

Table S9 Energy levels (cm^{-1}) of ligand field multiplets in zero field derived from ORCA/CASSCF computed for complex **2**.

Fig. S1 PXRD patterns for complexes **1** (a) and **2** (b).

Fig. S2 3D supramolecular networks of complex **1** (H atoms are deleted for clarity).

Fig. S3 3D supramolecular networks of complex **2** (H atoms and free H_2O molecules are deleted for clarity).

Fig. S4 M versus H at different temperatures.

Fig. S5 Ac magnetic susceptibility measurements for **1** (a) and **2** (b) in 0 Oe static field.

Fig. S6 Field dependence of the magnetic relaxation time at 2 K for **2**.

Fig. S7 Cole–Cole plots under 2000 Oe for **2**.

Table S1 Selected crystallographic data for complexes **1** and **2**.

| Complex | 1 | 2 |
|--|---|---|
| Empirical formula | C ₂₄ H ₂₂ CoN ₁₆ O ₂ | C ₂₄ H ₂₂ CoN ₁₈ O |
| Formula weight | 625.50 | 637.52 |
| Temperature | 100 K | 100 K |
| Crystal system | monoclinic | monoclinic |
| Space group | <i>P</i> 21/ <i>n</i> | <i>P</i> 21/ <i>n</i> |
| <i>a</i> (Å) | 7.7569(6) | 13.1218(7) |
| <i>b</i> (Å) | 15.7881(12) | 14.2515(7) |
| <i>c</i> (Å) | 10.9425(11) | 14.6292(8) |
| α (°) | 90 | 90 |
| β (°) | 91.562(8) | 102.327(5) |
| γ (°) | 90 | 90 |
| <i>V</i> (Å ³) | 1339.59(19) | 2672.7(2) |
| <i>Z</i> | 2 | 4 |
| <i>D</i> (g/cm ³) | 1.551 | 1.584 |
| <i>Mu</i> (mm ⁻¹) | 0.698 | 0.701 |
| <i>F</i> (0 0 0) | 642 | 1308 |
| Unique reflections | 3171 | 4557 |
| Observed reflections | 6107 | 6389 |
| <i>R</i> _{int} | 0.0536 | 0.0433 |
| Final <i>R</i> indices [<i>I</i> > 2σ(<i>I</i>)] | <i>R</i> ₁ = 0.0687 <i>wR</i> ₂ = 0.1284 | <i>R</i> ₁ = 0.0595 <i>wR</i> ₂ = 0.1223 |
| <i>R</i> indices (all data) | <i>R</i> ₁ = 0.1142 <i>wR</i> ₂ = 0.1558 | <i>R</i> ₁ = 0.0927 <i>wR</i> ₂ = 0.1386 |
| Goodness-of-fit on <i>F</i> ² | 1.060 | 1.060 |

Table S2 Selected Bond Lengths (Å) and Bond Angles (°) for **1**

| | 1 | | |
|----------------|----------|-------------------|-----------|
| Co(1)-O(1) | 2.043(2) | O(1)-Co(1)-O(1)#1 | 180 |
| Co(1)-O(1)#1 | 2.043(2) | O(1)-Co(1)-N(1) | 91.75(12) |
| Co(1)-N(1) | 2.175(3) | O(1)-Co(1)-N(6) | 94.71(12) |
| Co(1)-N(1)#1 | 2.175(3) | O(1)-Co(1)-N(1)#1 | 88.25(12) |
| Co(1)-N(6) | 2.131(3) | O(1)-Co(1)-N(6) | 85.29(12) |
| Co(1)-N(6)#1 | 2.131(3) | N(1)-Co(1)-N(6) | 92.28(13) |
| #1 1-x,1-y,-z; | | | |

Table S3 Selected Bond Lengths (\AA) and Bond Angles ($^\circ$) for **2**

| 2 | | | |
|-------------|----------|------------------|------------|
| Co(1)-N(5) | 2.096(3) | N(5)-Co(1)-N(6) | 77.29(10) |
| Co(1)-N(6) | 2.136(3) | N(5)-Co(1)-N(7) | 103.01(10) |
| Co(1)-N(7) | 2.143(3) | N(5)-Co(1)-N(8) | 176.49(10) |
| Co(1)-N(8) | 2.092(3) | N(6)-Co(1)-N(7) | 178.95(10) |
| Co(1)-N(13) | 2.144(3) | N(6)-Co(1)-N(8) | 102.61(10) |
| Co(1)-N(16) | 2.120(3) | N(6)-Co(1)-N(16) | 93.34(10) |

Table S4 Co(II) ion geometry analysis of **1** and **2** by SHAPE 2.1 software

| Configuration | ABOXIY, 1 | ABOXIY, 2 |
|---------------|------------------|------------------|
| OC-6 | 0.219 | 0.886 |
| TPR-6 | 15.903 | 15.162 |
| JPPY-6 | 32.199 | 30.312 |

Table S5 Relaxation fitting parameters from least-squares fitting of $\chi(f)$ data under 2000 Oe dc field of **2**

| T(K) | χ_T | χ_S | α |
|------|----------|----------|----------|
| 2 | 0.359 | 0.001 | 0.334 |
| 2.5 | 0.316 | 0.002 | 0.333 |
| 3 | 0.280 | 0.004 | 0.330 |
| 4 | 0.227 | 0.0004 | 0.306 |

Table S6 ORCA/CASSCF computed Individual contributions to *D*-tensor for complex **1**

| 2S+1 | Root | <i>D</i> | <i>E</i> | 2S+1 | Root | <i>D</i> | <i>E</i> |
|------|------|----------|----------|------|------|----------|----------|
| 4 | 0 | 0.000 | -0.000 | 2 | 15 | -0.207 | 0.299 |
| 4 | 1 | -83.460 | 0.028 | 2 | 16 | 0.833 | 0.017 |
| 4 | 2 | 19.085 | -19.221 | 2 | 17 | 0.013 | 0.008 |
| 4 | 3 | 6.156 | 6.175 | 2 | 18 | -0.948 | 0.959 |
| 4 | 4 | -9.218 | 0.455 | 2 | 19 | 0.011 | -0.120 |
| 4 | 5 | 0.081 | -0.204 | 2 | 20 | -0.529 | -0.560 |
| 4 | 6 | -0.002 | 0.000 | 2 | 21 | -0.132 | 0.044 |
| 4 | 7 | 0.066 | -0.069 | 2 | 22 | 0.512 | -0.019 |
| 4 | 8 | -0.011 | -0.002 | 2 | 23 | -0.054 | 0.070 |
| 4 | 9 | -0.132 | -0.002 | 2 | 24 | -0.121 | 0.137 |
| 2 | 0 | -4.522 | 4.579 | 2 | 25 | 0.001 | -0.018 |
| 2 | 1 | -0.306 | -1.141 | 2 | 26 | 0.470 | -0.016 |

| | | | | | | | |
|---|----|--------|--------|---|----|--------|--------|
| 2 | 2 | -0.018 | 0.018 | 2 | 27 | -0.013 | 0.014 |
| 2 | 3 | 2.448 | 0.006 | 2 | 28 | 0.051 | -0.019 |
| 2 | 4 | -0.006 | 0.012 | 2 | 29 | 0.084 | -0.006 |
| 2 | 5 | 0.001 | 0.004 | 2 | 30 | -0.069 | -0.090 |
| 2 | 6 | -0.004 | 0.001 | 2 | 31 | -0.043 | 0.051 |
| 2 | 7 | -1.247 | 1.282 | 2 | 32 | 0.009 | 0.003 |
| 2 | 8 | -1.653 | -1.654 | 2 | 33 | 0.130 | 0.003 |
| 2 | 9 | 0.190 | -0.001 | 2 | 34 | -0.001 | 0.002 |
| 2 | 10 | 0.032 | 0.001 | 2 | 35 | -0.005 | -0.018 |
| 2 | 11 | -0.063 | 0.061 | 2 | 36 | -0.009 | 0.010 |
| 2 | 12 | -0.335 | -0.355 | 2 | 37 | -0.002 | -0.004 |
| 2 | 13 | 0.158 | 0.098 | 2 | 38 | -0.003 | 0.000 |
| 2 | 14 | 0.013 | 0.000 | 2 | 39 | -0.064 | 0.063 |

Table S7 Energy levels (cm^{-1}) of ligand field multiplets in zero field derived from ORCA/CASSCF computed for complex **1**

| | | | | | | | |
|----|---------|----|---------|----|---------|-----|---------|
| 0 | 0.0 | 30 | 18780.6 | 60 | 24790.2 | 90 | 37725.9 |
| 1 | 0.0 | 31 | 18780.6 | 61 | 24790.2 | 91 | 37725.9 |
| 2 | 164.8 | 32 | 19285.7 | 62 | 26368.9 | 92 | 37939.5 |
| 3 | 164.8 | 33 | 19285.7 | 63 | 26368.9 | 93 | 37939.5 |
| 4 | 769.1 | 34 | 19427.8 | 64 | 28666.3 | 94 | 38368.5 |
| 5 | 769.1 | 35 | 19427.8 | 65 | 28666.3 | 95 | 38368.5 |
| 6 | 992.2 | 36 | 19841.6 | 66 | 29153.5 | 96 | 43017.1 |
| 7 | 992.2 | 37 | 19841.6 | 67 | 29153.5 | 97 | 43017.1 |
| 8 | 1843.4 | 38 | 19940.4 | 68 | 29433.0 | 98 | 43419.9 |
| 9 | 1843.4 | 39 | 19940.4 | 69 | 29433.0 | 99 | 43419.9 |
| 10 | 1894.1 | 40 | 20121.9 | 70 | 29796.0 | 100 | 43846.6 |
| 11 | 1894.1 | 41 | 20121.9 | 71 | 29796.0 | 101 | 43846.6 |
| 12 | 9032.3 | 42 | 20216.3 | 72 | 30744.6 | 102 | 45607.9 |
| 13 | 9032.3 | 43 | 20216.3 | 73 | 30744.6 | 103 | 45607.9 |
| 14 | 9079.8 | 44 | 21988.7 | 74 | 30961.0 | 104 | 46089.6 |
| 15 | 9079.8 | 45 | 21988.7 | 75 | 30961.0 | 105 | 46089.6 |
| 16 | 9972.6 | 46 | 22274.2 | 76 | 31947.6 | 106 | 46417.3 |
| 17 | 9972.6 | 47 | 22274.2 | 77 | 31947.6 | 107 | 46417.3 |
| 18 | 9992.9 | 48 | 22847.9 | 78 | 33246.4 | 108 | 46475.3 |
| 19 | 9992.9 | 49 | 22847.9 | 79 | 33246.4 | 109 | 46475.3 |
| 20 | 10294.6 | 50 | 23111.3 | 80 | 35028.5 | 110 | 65756.9 |

| | | | | | | | |
|----|---------|----|---------|----|---------|-----|---------|
| 21 | 10294.6 | 51 | 23111.3 | 81 | 35028.5 | 111 | 65756.9 |
| 22 | 10367.8 | 52 | 23464.8 | 82 | 35484.2 | 112 | 66580.2 |
| 23 | 10367.8 | 53 | 23464.8 | 83 | 35484.2 | 113 | 66580.2 |
| 24 | 10686.8 | 54 | 23767.7 | 84 | 36019.8 | 114 | 66827.8 |
| 25 | 10686.8 | 55 | 23767.7 | 85 | 36019.8 | 115 | 66827.8 |
| 26 | 11342.9 | 56 | 24145.9 | 86 | 36901.4 | 116 | 67270.9 |
| 27 | 11342.9 | 57 | 24145.9 | 87 | 36901.4 | 117 | 67270.9 |
| 28 | 18413.4 | 58 | 24473.5 | 88 | 37644.3 | 118 | 67642.5 |
| 29 | 18413.4 | 59 | 24473.5 | 89 | 37644.3 | 119 | 67642.5 |

Table S8 ORCA/CASSCF computed Individual contributions to D-tensor for complex 2

| 2S+1 | Root | D | E | 2S+1 | Root | D | E |
|------|------|---------|---------|------|------|--------|--------|
| 4 | 0 | 0.000 | -0.000 | 2 | 15 | 0.005 | 0.004 |
| 4 | 1 | -42.394 | -0.018 | 2 | 16 | 0.480 | -0.001 |
| 4 | 2 | 12.210 | -12.109 | 2 | 17 | 0.108 | -0.000 |
| 4 | 3 | 5.828 | 5.678 | 2 | 18 | -1.068 | 1.068 |
| 4 | 4 | -4.965 | -0.010 | 2 | 19 | -0.033 | -0.035 |
| 4 | 5 | -3.339 | -0.013 | 2 | 20 | -0.707 | -0.689 |
| 4 | 6 | 0.006 | -0.006 | 2 | 21 | 0.284 | -0.007 |
| 4 | 7 | 0.063 | -0.063 | 2 | 22 | 0.058 | 0.001 |
| 4 | 8 | -0.168 | -0.001 | 2 | 23 | -0.020 | -0.004 |
| 4 | 9 | -0.020 | 0.000 | 2 | 24 | 0.560 | 0.051 |
| 2 | 0 | -4.187 | 4.188 | 2 | 25 | 0.044 | 0.118 |
| 2 | 1 | -1.906 | -1.094 | 2 | 26 | -0.007 | -0.010 |
| 2 | 2 | 0.000 | 0.000 | 2 | 27 | 0.016 | 0.000 |
| 2 | 3 | 2.072 | 0.001 | 2 | 28 | 0.211 | -0.001 |
| 2 | 4 | 0.243 | 0.000 | 2 | 29 | 0.007 | -0.000 |
| 2 | 5 | 0.030 | 0.003 | 2 | 30 | -0.090 | -0.084 |
| 2 | 6 | -0.076 | 0.057 | 2 | 31 | -0.077 | 0.075 |
| 2 | 7 | -1.338 | 1.348 | 2 | 32 | -0.001 | 0.002 |
| 2 | 8 | 0.450 | -0.025 | 2 | 33 | 0.086 | 0.003 |
| 2 | 9 | -1.836 | -1.836 | 2 | 34 | 0.023 | 0.002 |
| 2 | 10 | 0.036 | -0.002 | 2 | 35 | -0.031 | -0.031 |
| 2 | 11 | -0.073 | 0.071 | 2 | 36 | -0.001 | 0.001 |
| 2 | 12 | -0.200 | -0.130 | 2 | 37 | 0.001 | -0.000 |
| 2 | 13 | 0.717 | 0.013 | 2 | 38 | -0.010 | 0.009 |
| 2 | 14 | -0.165 | 0.192 | 2 | 39 | -0.054 | 0.055 |

Table S9 Energy levels (cm^{-1}) of ligand field multiplets in zero field derived from ORCA/CASSCF computed for complex **2**

| 0 | 0.0 | 30 | 18896.0 | 60 | 26060.5 | 90 | 39947.7 |
|----|---------|----|---------|----|---------|-----|---------|
| 1 | 0.0 | 31 | 18896.0 | 61 | 26060.5 | 91 | 39947.7 |
| 2 | 80.0 | 32 | 19295.9 | 62 | 27258.1 | 92 | 40088.2 |
| 3 | 80.0 | 33 | 19295.9 | 63 | 27258.1 | 93 | 40088.2 |
| 4 | 1511.1 | 34 | 19959.0 | 64 | 29244.3 | 94 | 40617.1 |
| 5 | 1511.1 | 35 | 19959.0 | 65 | 29244.3 | 95 | 40617.1 |
| 6 | 1615.4 | 36 | 20771.0 | 66 | 29806.2 | 96 | 43334.7 |
| 7 | 1615.4 | 37 | 20771.0 | 67 | 29806.2 | 97 | 43334.7 |
| 8 | 2967.5 | 38 | 21157.1 | 68 | 30362.5 | 98 | 44029.6 |
| 9 | 2967.5 | 39 | 21157.1 | 69 | 30362.5 | 99 | 44029.6 |
| 10 | 3008.2 | 40 | 21820.0 | 70 | 31060.0 | 100 | 44602.3 |
| 11 | 3008.2 | 41 | 21820.0 | 71 | 31060.0 | 101 | 44602.3 |
| 12 | 9818.1 | 42 | 21866.7 | 72 | 31929.3 | 102 | 46512 |
| 13 | 9818.1 | 43 | 21866.7 | 73 | 31929.3 | 103 | 46512 |
| 14 | 9831.5 | 44 | 22513.2 | 74 | 32473.0 | 104 | 47158.6 |
| 15 | 9831.5 | 45 | 22513.2 | 75 | 32473.0 | 105 | 47158.6 |
| 16 | 10047.5 | 46 | 22877.3 | 76 | 32698.8 | 106 | 47648.5 |
| 17 | 10047.5 | 47 | 22877.3 | 77 | 32698.8 | 107 | 47648.5 |
| 18 | 10944.3 | 48 | 23450.9 | 78 | 34974.5 | 108 | 47830.2 |
| 19 | 10944.3 | 49 | 23450.9 | 79 | 34974.5 | 109 | 47830.2 |
| 20 | 11481.4 | 50 | 23680.2 | 80 | 35806.5 | 110 | 65973.3 |
| 21 | 11481.4 | 51 | 23680.2 | 81 | 35806.5 | 111 | 65973.3 |
| 22 | 11562.1 | 52 | 24399.6 | 82 | 36769.2 | 112 | 66901.7 |
| 23 | 11562.1 | 53 | 24399.6 | 83 | 36769.2 | 113 | 66901.7 |
| 24 | 12206.4 | 54 | 25068.2 | 84 | 37225.0 | 114 | 68145.6 |
| 25 | 12206.4 | 55 | 25068.2 | 85 | 37225.0 | 115 | 68145.6 |
| 26 | 12294.4 | 56 | 25289.4 | 86 | 38076.5 | 116 | 68496.4 |
| 27 | 12294.4 | 57 | 25289.4 | 87 | 38076.5 | 117 | 68496.4 |
| 28 | 18213.1 | 58 | 25833.5 | 88 | 39002.3 | 118 | 68722.5 |
| 29 | 18213.1 | 59 | 25833.5 | 89 | 39002.3 | 119 | 68722.5 |

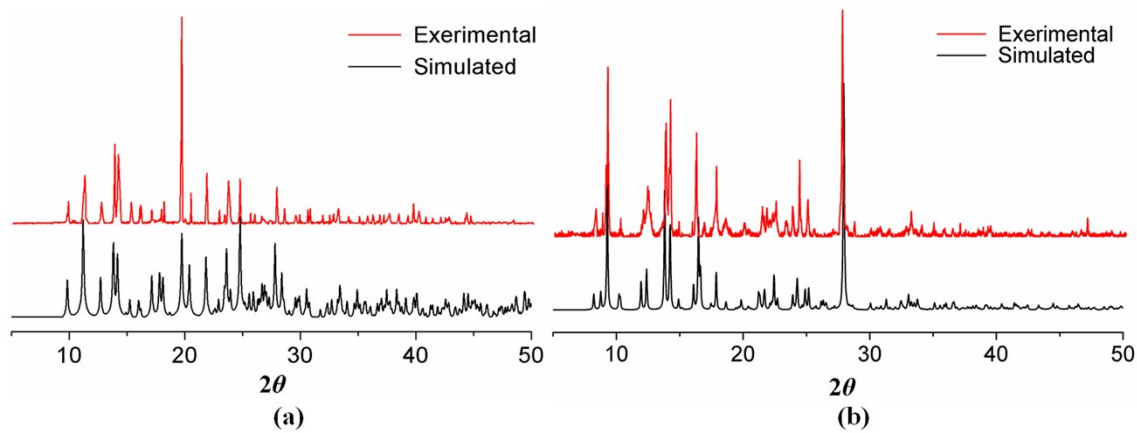


Fig. S1 PXRD patterns for complexes **1** (a) and **2** (b).

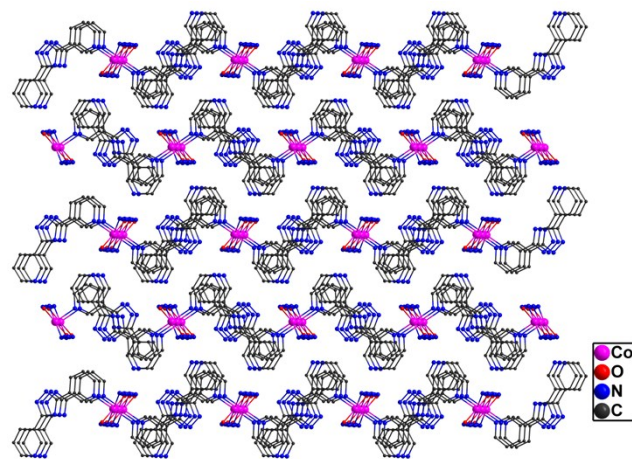


Fig. S2 3D supramolecular networks of complex **1** (H atoms have been deleted for clarity).

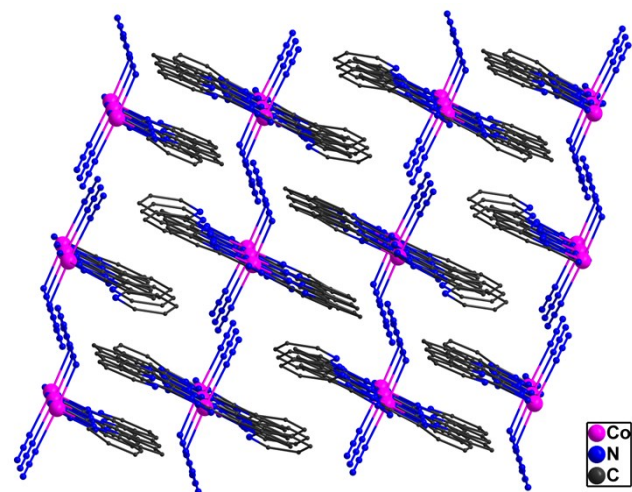


Fig. S3 3D supramolecular networks of complex **2** (H atoms have been deleted for clarity).

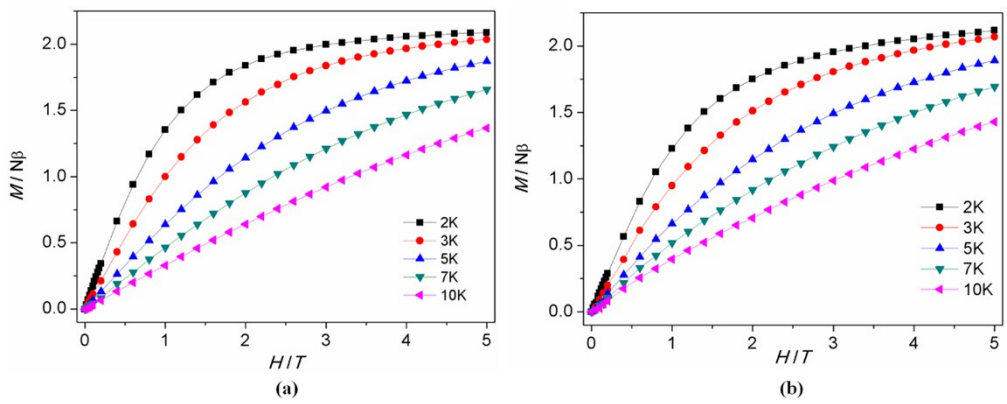


Fig. S4 M versus H at different temperatures.

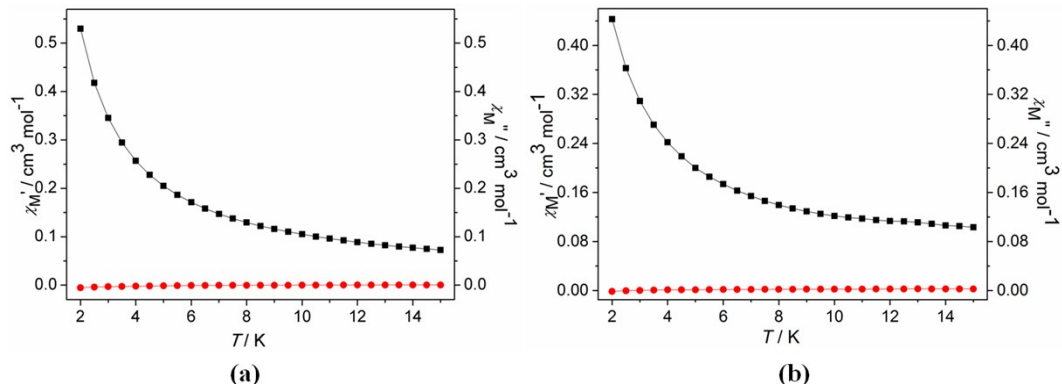


Fig. S5 Ac magnetic susceptibility measurements for **1** (a) and **2** (b) in 0 Oe static field.

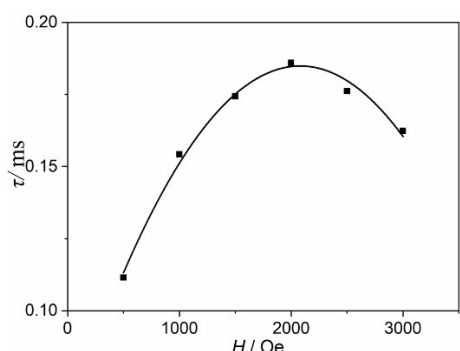


Fig. S6 Field dependence of the magnetic relaxation time at 2 K for **2**.

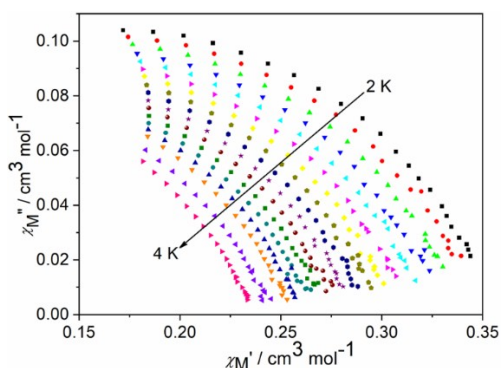


Fig. S7 Cole–Cole plots under 2000 Oe for **2**.